ANTIOXIDANTS & REDOX SIGNALING
Volume 22, Number 1, 2015

DOI: 10.1089/ars.2013.5748

Discoveries

ORIGINAL RESEARCH COMMUNICATION

Peroxiredoxin II Negatively Regulates Lipopolysaccharide-Induced Osteoclast Formation and Bone Loss *via* JNK and STAT3

Hyojung Park,[1] A Long Sae Mi Noh,[1] Ju-Hee Kang,[1] Jung-Sun Sim,[1] Dong-Seok Lee,[2] and Mijung Yim[1]

Abstract

Aims: Lipopolysaccharide (LPS) is considered a prominent pathogenic factor in inflammatory bone diseases. LPS challenge contributes to the production of reactive oxygen species (ROS) in diverse inflammatory diseases. However, its mechanism remains to be clarified in bone. Thus, we investigated the critical mechanism of ROS in LPS-induced osteoclastogenesis and bone loss. ***Results:*** Antioxidant prevented LPS-induced osteoclast formation *via* inhibition of nuclear factor of activated T-cells, cytoplasmic 1 (NFATc1) and c-Fos expression in preosteoclasts. Moreover, LPS-induced osteoclast formation *via* ROS was attenuated by treatment with c-Jun N-terminal protein kinase (JNK) inhibitor. Interestingly, LPS also activated signal transducer and activator of transcription 3 (STAT3), which is suppressed by antioxidants. We found that knockdown of STAT3 or use of a STAT3 inhibitor resulted in a significant reduction in interleukin-1 beta (IL-1β), interleukin-6 (IL-6), and nitric oxide (NO) production, followed by decreased osteoclast formation by LPS. Peroxiredoxin II (PrxII) is a member of the antioxidant enzyme family, and it plays a protective role against oxidative damage caused by ROS. In our study, ROS production and osteoclast formation by LPS was significantly enhanced in PrxII$^{-/-}$ cells. Moreover, JNK-mediated c-Fos and NFATc1 expression was promoted in PrxII$^{-/-}$ cells. Furthermore, STAT3 activation and accompanying IL-1β, IL-6, and NO production was also increased in PrxII$^{-/-}$ cells. Consistent with the *in vitro* result, PrxII-deficient mice showed increased osteoclast formation and bone loss by LPS challenge compared with wild-type mice. ***Innovation:*** For the first time, we showed that LPS-induced ROS signaling is dependent on the coordinated mechanism of JNK and STAT3 during osteoclastogenesis, which is negatively regulated by PrxII. ***Conclusion:*** We suggest that PrxII could be useful in the development of a novel target for inflammatory bone loss. *Antioxid. Redox Signal.* 22, 63–77.

Introduction

THE SKELETON IS A METABOLICALLY active organ that undergoes continuous remodeling throughout life. Bone remodeling is the restructuring process of existing bone, which undergoes constant resorption and formation. Bone resorption is essential for calcium homeostasis and bone remodeling. However, excessive resorption is the cause of bone loss observed in common diseases such as postmenopausal osteoporosis, rheumatoid arthritis, and periodontitis (15). Osteoclasts are tartrate-resistant acid phosphatase (TRAP)-

Innovation

Lipopolysaccharide (LPS) is a critical pathogenic factor in inflammatory bone diseases. In this work, we verified that peroxiredoxin II (PrxII)-mediated reactive oxygen species production regulates LPS-induced osteoclast formation and bone loss *via* c-Jun N-terminal protein kinase (JNK) and signal transducer and activator of transcription 3 (STAT3) pathway. These findings suggest that PrxII is an important regulator for inflammatory bone loss.

[1]College of Pharmacy, Sookmyung Women's University, Seoul, Republic of Korea.
[2]College of Natural Sciences, Kyungpook National University, Daegu, Republic of Korea.

positive multinucleated cells (MNCs) with bone resorbing activity and are differentiated from hematopoietic cells through a multi-step process, including proliferation, expression of TRAP, and fusion of cells (49). Receptor activator of nuclear factor-kappaB ligand (RANKL) is an essential osteoclastogenesis-inducing factor that is expressed as a membrane-bound and a secreted protein by osteoblasts (6, 21, 49). Osteoclast precursors recognize RANKL through RANK, a receptor of RANKL, and then differentiate into osteoclasts in the presence of macrophage-colony-stimulating factor (M-CSF). Furthermore, the binding of RANKL to its receptor results in the recruitment of the TNF receptor-associated factor (TRAF) family of protein, for example, TRAF-6, which activates nuclear factor-kappaB (NF-κB), c-Jun N-terminal kinase (JNK), extracellular signal-regulated kinase 1/2 (ERK1/2), and p38 mitogen-activated protein kinase (MAPK), and, eventually, leads to the proliferation, differentiation, and maturation of osteoclasts (31).

Lipopolysaccharide (LPS) is an important component of the outer membrane of Gram-negative bacteria. LPS plays an important role in bone loss by initiating a local host response that involves recruitment of inflammatory cells, production of prostanoids and cytokines, elaboration of lytic enzymes, and activation of osteoclast formation and function (16, 35, 36). By using the C3H/HeJ mouse strain, which has a defective response to LPS, toll-like receptor 4 (TLR4) has been demonstrated to be an important sensor for LPS (40). On LPS recognition, TLR4 undergoes oligomerization and recruits its downstream adaptors through interactions with toll-interleukin-1 receptor (TIR) domains in order to propagate the signal. Adapter molecules, including myeloid differentiation primary response gene 88 (MyD88), toll-interleukin 1 receptor domain containing adaptor protein (Tirap), TIR-domain-containing adapter-inducing interferon-β (Trif), and TRIF-related adaptor molecule (Tram), are known to be involved in signaling (20, 55, 56). The adapters activate other molecules within the cell, leading to induction of the inflammatory response. Recent experimental evidence has shown that LPS-mediated inflammation is highly dependent on reactive oxygen species (ROS) and associated signaling pathways, such as the p38 MAPK, JNK, and ERK cascades (39, 48, 52).

ROS act as second messengers in signal transduction and gene regulation in a variety of cell types and under several biological conditions such as cytokine, growth factor, and hormone treatments, ion transport, transcription, neuromodulation, and apoptosis (15, 17, 30). ROS are mainly represented by the superoxide radical anion ($O_2^{\bullet -}$), hydrogen peroxide (H_2O_2), and the hydroxyl radical ($OH^{\bullet}$) in cells. It is now well established that H_2O_2 is the main ROS-mediating cellular signaling because of its capacity to inhibit tyrosine phosphatases through oxidation of cysteine residues in their catalytic domains, which, in turn, activates tyrosine kinases and downstream signaling (2, 51). Under normal circumstances, cells are able to defend themselves against ROS damage with enzymes such as superoxide dismutases, catalases, glutathione peroxidases, glutathione reductase, and peroxiredoxins (Prxs) (13, 34, 53). Among them, Prxs constitute a family of multifunctional antioxidant thiol-dependent peroxidases that have been identified in a large variety of organisms, such as bacteria, yeast, plants, and mammals. They act as scavengers of hydrogen peroxide using reducing equivalents provided by thiol-containing proteins such as thioredoxin (43). The mammalian Prx family members can be divided into six distinct groups (types I through VI). One of the Prx family members PrxII (gene loci, *PrdxII*), which belongs to the 2-cys Prx subfamily, is a prime candidate for a regulator of H_2O_2 signaling initiated by cell-surface receptors (7, 23, 32). Since PrxII recently has been identified as an essential negative regulator of LPS-induced inflammatory signaling (57), we investigated whether PrxII regulates LPS-induced osteoclastogenesis. In this study, we demonstrated that PrxII is involved in LPS-induced osteoclastogenesis through modulation of ROS signaling.

Results

LPS induces osteoclast formation via *ROS-mediated JNK signaling pathway*

LPS promotes osteoclastogenesis from RANKL-primed precursors *in vitro* (22, 59). LPS induces the activation of multiple intracellular signals that are essential for osteoclastogenesis, including NF-κB, p38, ERK1/2, and JNK (20). These signals lead to osteoclast differentiation through two essential transcription factors, c-Fos and nuclear factor of activated T-cells, cytoplasmic 1 (NFATc1) (50). To verify the role of ROS in LPS-induced osteoclast formation, we assessed the effect of antioxidant *N*-acetyl-cysteine (NAC) using RANKL-primed precursors as preosteoclasts. When preosteoclasts were treated with LPS for 4 days, numerous tartrate-resistant acid phosphatase (TRAP)-positive multinucleated osteoclasts were generated. Treatment with NAC significantly attenuated the LPS-induced osteoclast formation (Fig. 1A), suggesting that LPS mediates ROS to induce osteoclast formation. We also found that NAC completely blocked LPS-induced NFATc1 and c-Fos expression (Fig. 1B, C). Since NAC prevented LPS-induced activation of JNK (Fig. 1D), we examined the involvement of JNK in LPS-induced osteoclast formation. JNK inhibitor decreased osteoclast formation by LPS in a dose-dependent manner (Fig. 1E). Furthermore, JNK inhibitor attenuated NFATc1 and c-Fos expression (Fig. 1F, G). These results indicate that ROS mediate LPS-induced osteoclastogenesis *via* JNK.

LPS activates STAT3 via *ROS to induce osteoclast formation*

Signal transducer and activator of transcription 3 (STAT3) is one of the six members of a family of transcription factors. STAT3 is activated through phosphorylation at two residues, tyrosine 705 and serine 727. Since STAT3 plays an important role in LPS-induced inflammation (45), we investigated the involvement of STAT3 in LPS-induced osteoclast formation. First, we investigated whether LPS activates STAT3 *via* TLR4 in preosteoclasts using C3H/HeJ mice, which possess a missense mutation in TLR4 gene (40). LPS increased the level of phospho-tyrosine^{705} and phospho-serine^{727} STAT3 in cells from C3H/HeN (normal mice), but not in cells from C3H/HeJ mice (Fig. 2A, B). Next, we examined whether LPS activates STAT3 *via* ROS in preosteoclasts. We found that phosphorylation of STAT3 by LPS was efficiently blocked by NAC (Fig. 2C, D). To examine whether STAT3 is involved in LPS-induced osteoclastogenesis, we used the STAT3 inhibitor, stattic, and small interfering RNA (siRNA)

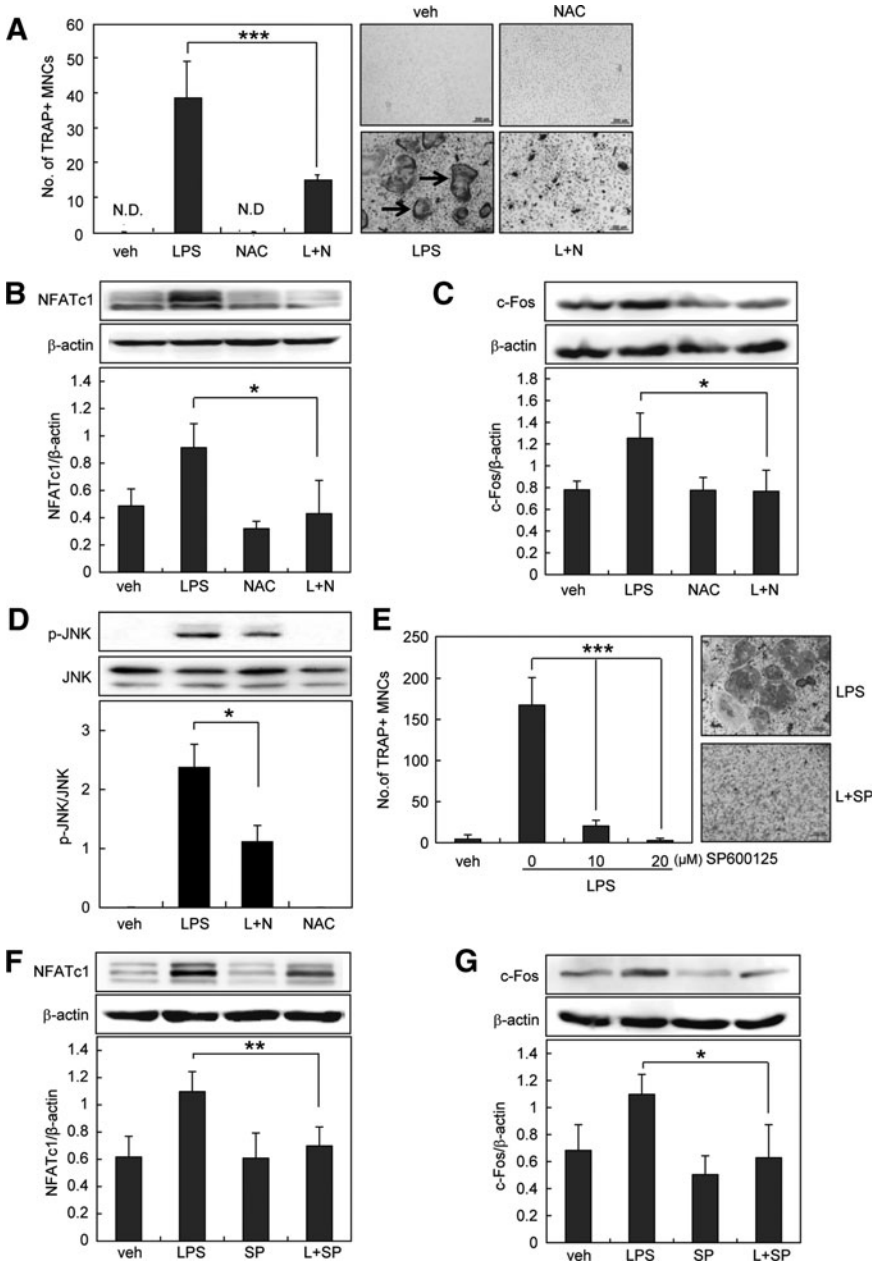

FIG. 1. Antioxidant inhibits LPS-induced osteoclastogenesis *via* JNK signaling pathways. (A, E) Pre-osteoclasts were treated with 1 μg/ml LPS in the absence or presence of NAC (antioxidant, 20 m*M*) or SP600125 (JNK inhibitor, 20 μ*M*). On day 4, cells were fixed and stained for TRAP. Cell morphology was examined by light microscopy, and TRAP-positive MNCs having more than three nuclei (*arrows*) were counted. **(B–D, F, G)** Pre-osteoclasts were serum starved for 12 h and stimulated with 1 μg/ml LPS in the absence or presence of NAC (20 m*M*) or SP600125 (20 μ*M*). After 24 h, whole-cell extracts were harvested from cultured cells and subjected to SDS-PAGE and Western blot analysis to detect p-JNK, NFATc1, or c-Fos. Antibodies specific for JNK and β-actin were used to normalize the cell extracts. All values are the mean ± SD of three independent experiments. $*p < 0.05$, $**p < 0.01$, and $***p < 0.005$; scale bar = 200 μm. JNK, c-Jun N-terminal protein kinase; LPS, lipopolysaccharide; MNCs, multinucleated cells; NAC, *N*-acetyl-cysteine; NFATc1, nuclear factor of activated T-cells, cytoplasmic 1; SD, standard deviation; SDS-PAGE, sodium dodecyl sulfate–polyacrylamide gel electrophoresis; TRAP, tartrate-resistant acid phosphatase.

targeting STAT3. As shown in Figure 3A, stattic (1 μ*M*) reduced the formation of TRAP-positive MNCs. Stattic at this concentration did not affect cell viability or morphology. In addition, the knockdown of STAT3 with specific siRNA reduced the formation of multinucleated osteoclasts (Fig. 3B). Taken together, these results suggest that LPS activates STAT3 *via* ROS, which mediates osteoclast formation.

STAT3 modulates IL-1β, IL-6, and NO production to mediate osteoclast formation by LPS.

Osteoclast development and activity are increased by various pro-inflammatory cytokines such as interleukin-1 beta (IL-1β) and interleukin-6 (IL-6) (18, 24, 25, 27, 29, 44, 58). To verify the precise mechanism by which STAT3 mediates LPS-induced osteoclast formation, we examined the involvement of IL-1β and IL-6. We found that STAT3 inhibitor decreased IL-1β and IL-6 expression by LPS in pre-osteoclasts (Fig. 3C, D). The reduction in the production of IL-1β and IL-6 by STAT3 inhibitor was also confirmed by enzyme-linked immunosorbent assay (ELISA) (Fig. 3E, F). Inducible nitric oxide synthase (iNOS) is also known to mediate osteoclast formation through nitric oxide (NO) production (11, 14). When we further investigated the involvement of iNOS and NO, STAT3 inhibitor was shown to attenuate LPS-induced iNOS expression and NO production (Fig. 3G, H). Similar to STAT3 inhibitor, STAT3-specific siRNA significantly reduced NO production as well as the production of IL-1β and IL-6 compared with nontargeting control siRNA (Fig. 3I–3K). Taken together, these results suggest that STAT3 activation by LPS stimulates IL-1β, IL-6, and NO production, which leads to osteoclastogenesis.

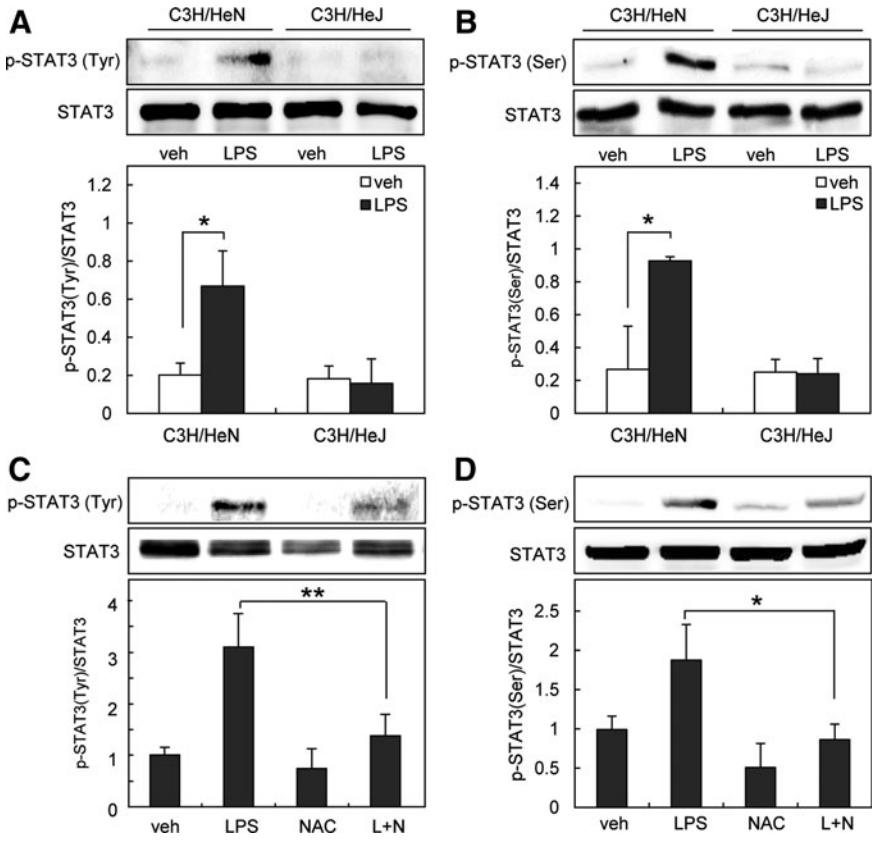

FIG. 2. Antioxidant prevents STAT3 activation during LPS-induced osteoclastogenesis. (A, B) Preosteoclasts from toll-like receptor-4-mutant (C3H/HeJ) and wild-type (C3H/HeN) mice were serum starved for 12 h and stimulated with 1 μg/ml LPS. **(C, D)** Preosteoclasts were serum starved for 12 h and stimulated with 1 μg/ml LPS in the absence or presence of NAC (20 m*M*). Whole-cell extracts were harvested from cultured cells and subjected to SDS-PAGE and Western blot analysis to detect phosphorylated STAT3 at Tyr705 **(A, C)** or Ser727 **(B, D)**. Antibodies specific for STAT3 were used to normalize the cell extracts. All values are the mean ± SD of three independent experiments. $*p < 0.05$, $**p < 0.01$. STAT3, signal transducer and activator of transcription 3.

PrxII deficiency facilitates LPS-induced osteoclast formation

PrxII is a thiol-based peroxide reductase that clears cellular H_2O_2 and other free radicals to reduce cellular ROS (32). Since ROS mediates LPS-induced osteoclastogenesis, we verified the role of PrxII in LPS-induced osteoclastogenesis using $PrxII^{-/-}$ mice. First, we measured the amount of intracellular ROS in preosteoclasts. On LPS stimulation, $PrxII^{-/-}$ preosteoclasts produced significantly higher levels of ROS than $PrxII^{+/+}$ cells (Fig. 4A). Next, we examined the osteoclast differentiation using $PrxII^{+/+}$ and $PrxII^{-/-}$ cells. When preosteoclasts were treated with LPS, osteoclast formation was enhanced in PrxII-deficient cells in a dose-dependent manner (Fig. 4B). To examine whether the effect of PrxII on osteoclast formation could be reflected in the osteoclastic activity, we performed an *in vitro* resorption pit assay. Pit formation was accelerated in the wells of $PrxII^{-/-}$ cells treated with LPS (Fig. 4C). To further determine the role of PrxII in osteoclast differentiation, we examined the gene expression of cathepsin K (CTK), calcitonin receptor (CTR), dendritic cell-specific transmembrane protein (DC-STAMP), V-ATPase d2 (ATP6v0d2), and β3-integrin, all of which are marker genes of osteoclasts. Quantitative real-time polymerase chain reaction (PCR) analysis showed that LPS-induced expression levels of osteoclastic markers were promoted in PrxII-deficient cells, which is consistent with the increased osteoclastogenesis. (Fig. 4D). Furthermore, the overexpression of PrxII in preosteoclasts decreased LPS-induced osteoclast formation by 50% (Fig. 4E). These results clearly indicate that PrxII negatively regulates LPS-induced osteoclastogenesis *via* ROS.

PrxII regulates LPS-induced osteoclastogenesis through JNK-NFATc1 pathway

To investigate the molecular mechanism by which PrxII regulates LPS-induced osteoclastogenesis, we next examined the LPS-mediated signaling for osteoclastogenesis in PrxII-deficient cells. The transcription factor NFATc1 plays a central role in osteoclast formation, and its expression is regulated by c-Fos (50). We, therefore, examined the expression of c-Fos and NFATc1 induced by LPS. Western blot analysis revealed that PrxII deficiency promoted LPS-induced expression of NFATc1 and c-Fos (Fig. 5A, B). When we further investigated the osteoclastogenesis-related signaling, we found that JNK activation was significantly increased in response to LPS in $PrxII^{-/-}$ cells compared with $PrxII^{+/+}$ cells (Fig. 5C). No significant differences between $PrxII^{-/-}$ and $PrxII^{+/+}$ cells were observed in other signaling pathways such as ERK, p38, NF-κB, phospholipase-C gamma-1 (PLCγ-1), and cAMP response element-binding protein (CREB) (data not shown). These data revealed that PrxII negatively regulates LPS-induced osteoclastogenesis by hindering the JNK-NFATc1 pathway.

PrxII controls STAT3-mediated IL-1β, IL-6, and NO production during LPS-induced osteoclastogenesis

To further probe the signaling pathway linking PrxII to osteoclastogenesis, we tested whether PrxII modifies STAT3 activation during LPS-induced osteoclastogenesis. The phosphorylation of STAT3 at both Tyr705 and Ser727 was increased in $PrxII^{-/-}$ cells (Fig. 6A, B), indicating that

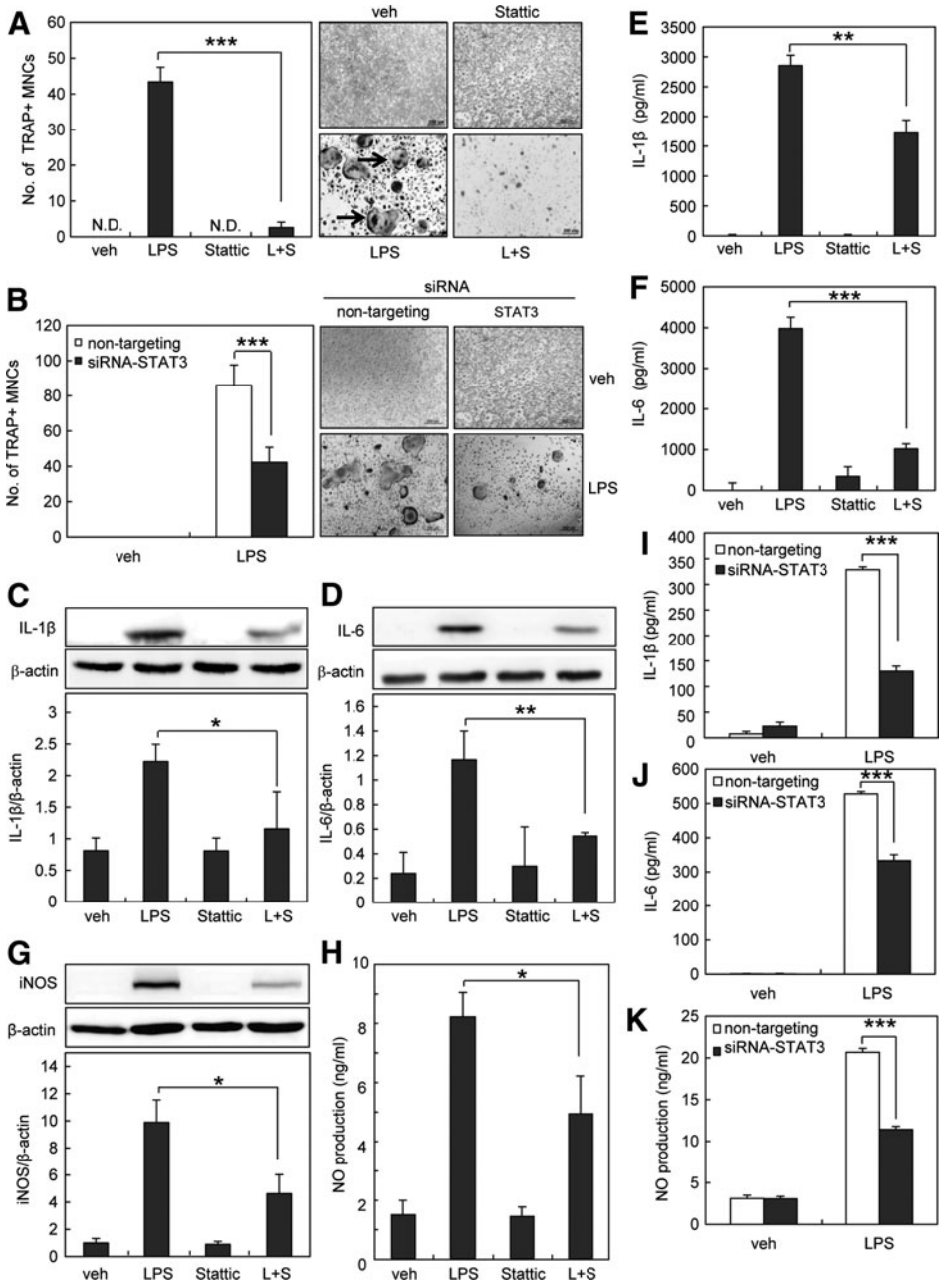

FIG. 3. Inhibition of STAT3 attenuates LPS-induced osteoclastogenesis by blocking IL-1β, IL-6, and NO production. **(A)** Preosteoclasts were treated with 1 μg/ml LPS in the absence or presence of stattic (STAT3 inhibitor, 1 μM). On day 4, cells were fixed and stained for TRAP, and TRAP-positive MNCs having more than three nuclei were counted. **(B)** One hundred nanomolars siRNA-transfected preosteoclasts were cultured for an additional 4 days with 1 μg/ml LPS. Cells were fixed and stained for TRAP, and TRAP-positive MNCs having more than three nuclei were counted. **(C, D)** Preosteoclasts were serum starved for 12 h and stimulated with 1 μg/ml LPS in the absence or presence of stattic (1 μM). After 6 h, whole-cell extracts were harvested from cultured cells and subjected to SDS-PAGE and Western blot analysis to detect IL-1β or IL-6. **(E, F)** Preosteoclasts were serum starved for 12 h and stimulated with 1 μg/ml LPS in the absence or presence of stattic (1 μM). The supernatants were harvested at 24 h. IL-1β and IL-6 concentration was measured in cell supernatants using ELISA. **(G)** Preosteoclasts were serum starved for 12 h and stimulated with 1 μg/ml LPS in the absence or presence of stattic (1 μM). After 24 h, whole-cell extracts were harvested from cultured cells and subjected to SDS-PAGE and Western blot analysis to detect iNOS expression. **(H)** Preosteoclasts were cultured for 4 days with 1 μg/ml LPS. Cell supernatants were harvested, and NO production was measured as nitrite using the Griess reagent. **(I–K)** One hundred nanomolars siRNA-transfected preosteoclasts were cultured for 24 h with 1 μg/ml LPS. IL-1β and IL-6 concentration was measured in cell supernatants using ELISA. The supernatant NO production was analyzed by the Griess method. The detection of β-actin in each sample serves as a loading control. All values are the mean $\pm$ SD of three independent experiments.*$p < 0.05$, **$p < 0.01$, and ***$p < 0.005$. ELISA, enzyme-linked immunosorbent assay; IL-1β, interleukin-1 beta; IL-6, interleukin-6; iNOS, inducible nitric oxide synthase; NO, nitric oxide; siRNA, small interfering RNA.

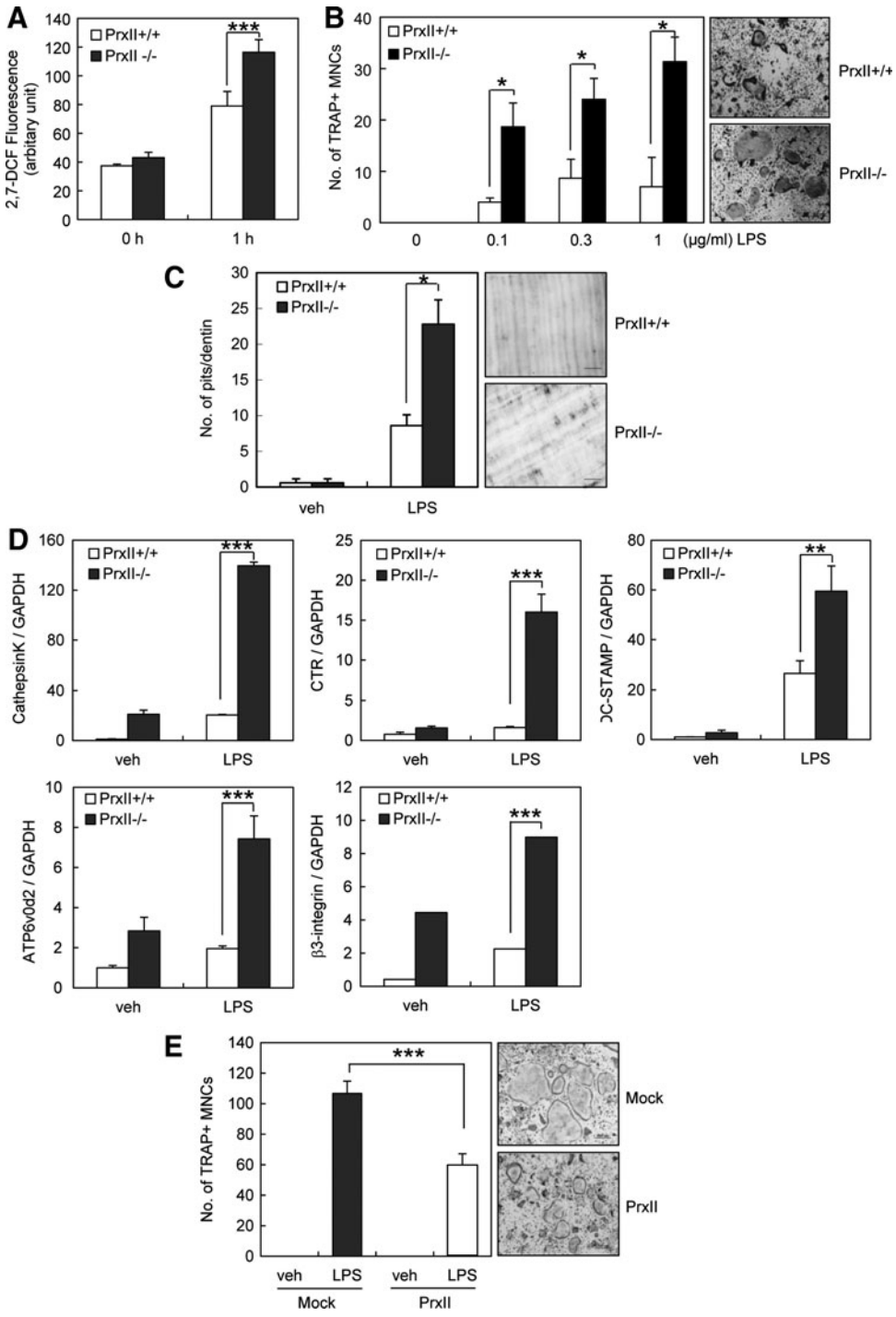

FIG. 4. PrxII deficiency enhances LPS-induced osteoclastogenesis. **(A)** Preosteoclasts were preloaded with 50 μM DCFH-DA and treated with 1 μg/ml LPS for 1 h. Intracellular ROS were measured by DCF fluorescence using a CytoFluor 4000 plate reader (488 nm excitation, 530 nm emission). **(B)** Preosteoclasts were incubated with 1 μg/ml LPS. On day 4, cells were fixed and stained for TRAP. The number of TRAP-positive MNCs having more than three nuclei was counted. **(C)** Preosteoclasts were placed on dentin slices and cultured with 1 μg/ml LPS for 6 days. The remaining cells were removed and stained with toluidine blue. The resorbed pit numbers were counted. **(D)** Preosteoclasts were incubated with 1 μg/ml LPS for 4 days. mRNA expression of various osteoclastogenic genes was determined by quantitative real-time PCR with GAPDH mRNA as an endogenous control. **(E)** Mock- and PrxII-transduced preosteoclasts were cultured with 1 μg/ml LPS for 4 days. Cells were fixed and stained for TRAP, and TRAP-positive MNCs having more than three nuclei were counted. Mock, pool of empty vector-transfected cells; PrxII, pool of cells overexpressing PrxII. All values are the mean ± SD of three independent experiments. $*p < 0.05$, $**p < 0.01$, and $***p < 0.005$. DCFH-DA, 2′,7′-dichlorofluorescin-diacetate; GAPDH, glyceraldehyde 3-phophate dehydrogenase; PCR, polymerase chain reaction; PrxII, peroxiredoxin II; ROS, reactive oxygen species.

PrxII regulates osteoclast formation by modulating STAT3 activation.

Since production of the pro-inflammatory cytokines IL-1β and IL-6 was affected by STAT3 (Fig. 3), we measured the levels of IL-1β and IL-6 in PrxII$^{-/-}$ and PrxII$^{+/+}$ preosteoclasts. We found that IL-1β and IL-6 production was enhanced in PrxII-deficient cells (Fig. 6C–F). Furthermore, iNOS expression and NO production were also enhanced in PrxII-deficient cells (Fig. 6G, H). These results showed that PrxII controls STAT3-mediated IL-1β, IL-6, and NO production during LPS-induced osteoclastogenesis.

PrxII$^{-/-}$ mice show increased osteoclast formation and bone loss when challenged by LPS

We next verified the role of PrxII *in vivo*. At first, we administered LPS to mouse calvaria to check osteoclast formation in two types of mice. Consistent with the *in vitro* study, LPS treatment led to more TRAP-stained osteoclast formation in PrxII$^{-/-}$ mice (Fig. 7A). Micro-CT analysis of calvariae demonstrated that PrxII$^{-/-}$ mice showed more severe bone destruction by LPS compared with PrxII$^{+/+}$ mice (Fig. 7B). We next examined the LPS-induced bone

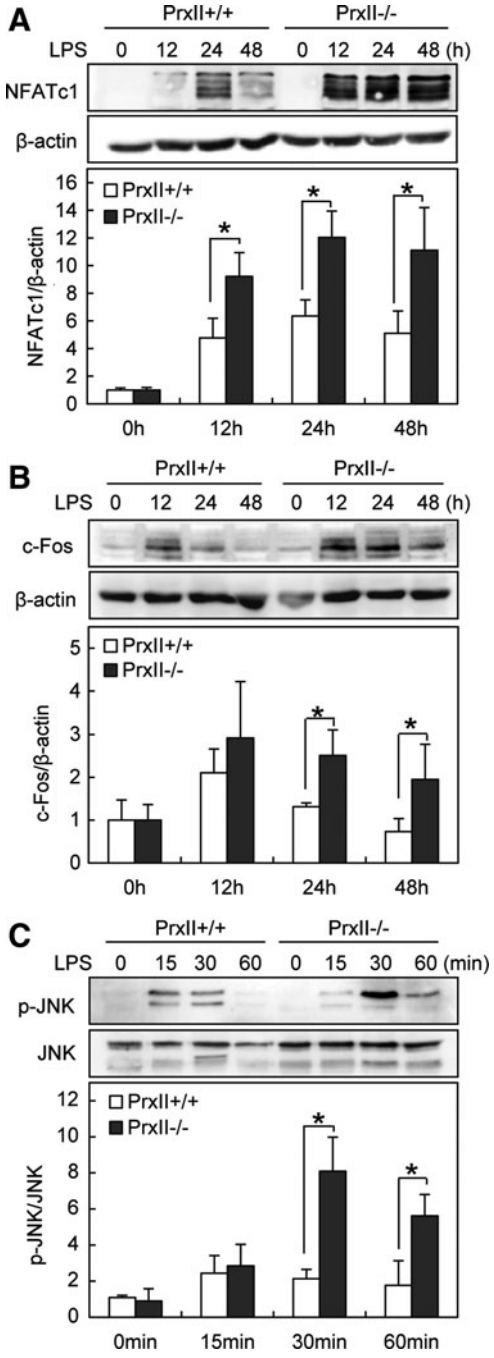

FIG. 5. PrxII deficiency enhances LPS-induced c-Fos and NFATc1 expression through JNK pathway. (A–C) Preosteoclasts were serum starved for 12 h and stimulated with 1 μg/ml LPS for the indicated time. Whole-cell extracts were harvested from cultured cells and subjected to SDS-PAGE and Western blot analysis to detect NFATc1, c-Fos, and p-JNK. The detection of β-actin and JNK in each sample serves as a loading control. All values are the mean ± SD of three independent experiments. $*p < 0.05$.

loss. PrxII$^{+/+}$ and PrxII$^{-/-}$ mice were injected i.p. twice with LPS over an 8-day period. Bone mineral density (BMD) of femur was measured by dual X-ray absorptiometry (DXA) analysis. While LPS treatment led to a significant bone loss in both PrxII$^{+/+}$ and PrxII$^{-/-}$ mice, PrxII$^{-/-}$ mice have significantly lower BMD (Fig. 8A). A micro-CT analysis of the metaphyseal region of the femur consistently showed that the trabecular bone volume per tissue volume (BV/TV) was significantly lower in PrxII$^{-/-}$ mice than in PrxII$^{+/+}$ mice after LPS injection (Fig. 8B). Two other indices related to BV/TV—the trabecular thickness (Tb.Th) and the trabecular number (Tb.N; linear density of trabecular bone)—were also reduced in PrxII$^{-/-}$ mice compared with PrxII$^{+/+}$mice after LPS injection (Fig. 8C, D). In addition, the higher structure model index (SMI) number, an indicator of increased fragility, was significantly increased in LPS-injected PrxII$^{-/-}$ mice, while the SMI of LPS-injected PrxII$^{+/+}$ mice was unchanged (Fig. 8E). Consistent with these results, three-dimensional visualization of the femoral area clearly showed that the massive loss of trabecular bone after LPS treatment was much higher in PrxII$^{-/-}$ mice compared with PrxII$^{+/+}$ mice (Fig. 8F). These results indicate that PrxII negatively regulates LPS-induced bone loss *via* modulation of osteoclast differentiation.

Discussion

Many kinds of inflammatory bone diseases are associated with excessive bone resorption induced by LPS (36). During inflammatory response, LPS significantly contributes to the production of ROS (4). Prxs are a class of thiol peroxidases that degrade hydroperoxides to water (42, 54). Catalase and glutathione peroxidases also remove hydroperoxides, and these enzymes have been considered the major enzymes that are responsible for protecting cells against hydroperoxides. However, recent data on the reactivity and abundance of the Prxs have revealed them to also be prominent members of the antioxidant defense network (41). Recently, the physiological role of PrxII in bone has been suggested (26). Deletion of PrxII causes a decrease in bone density possibly by increasing ROS concentration and calcium oscillation. Since the pathological role of PrxII in bone is poorly understood, we investigated the role of PrxII in ROS signaling during LPS-induced bone loss.

LPS accelerates osteoclast differentiation and activity (47). According to our results, ROS production was increased by LPS, and antioxidant inhibited LPS-induced osteoclast formation (Fig. 1). Furthermore, lack of PrxII increased osteoclast formation by LPS (Fig. 4). The increased LPS-induced osteoclastogenesis from PrxII-deficient pre-osteoclasts appears to be linked to the antioxidant activity of PrxII, given that the overall levels of ROS were significantly higher in PrxII-deficient cells after LPS stimulation than those in WT cells (Fig. 4). The overexpression of PrxII in preosteoclasts effectively but not completely attenuated LPS-induced osteoclast formation (Fig. 4). Given that six isoforms of Prxs (PrxI–VI) are expressed in preosteoclasts (data not shown), PrxII may act in balance with other Prxs in LPS-induced osteoclastogenesis.

Consistent with the increase in LPS-induced osteoclast formation, PrxII-deficient mice showed increased inflammatory bone loss *in vivo* (Figs. 7 and 8). Therefore, we concluded that the antioxidant enzyme PrxII negatively regulates LPS-induced bone loss *via* ROS signaling. ROS have many sources, including the mitochondrial electron transport chain, xanthine oxidase, cytochrome P-450 enzymes, uncoupled NO synthases, and NADPH oxidases. The

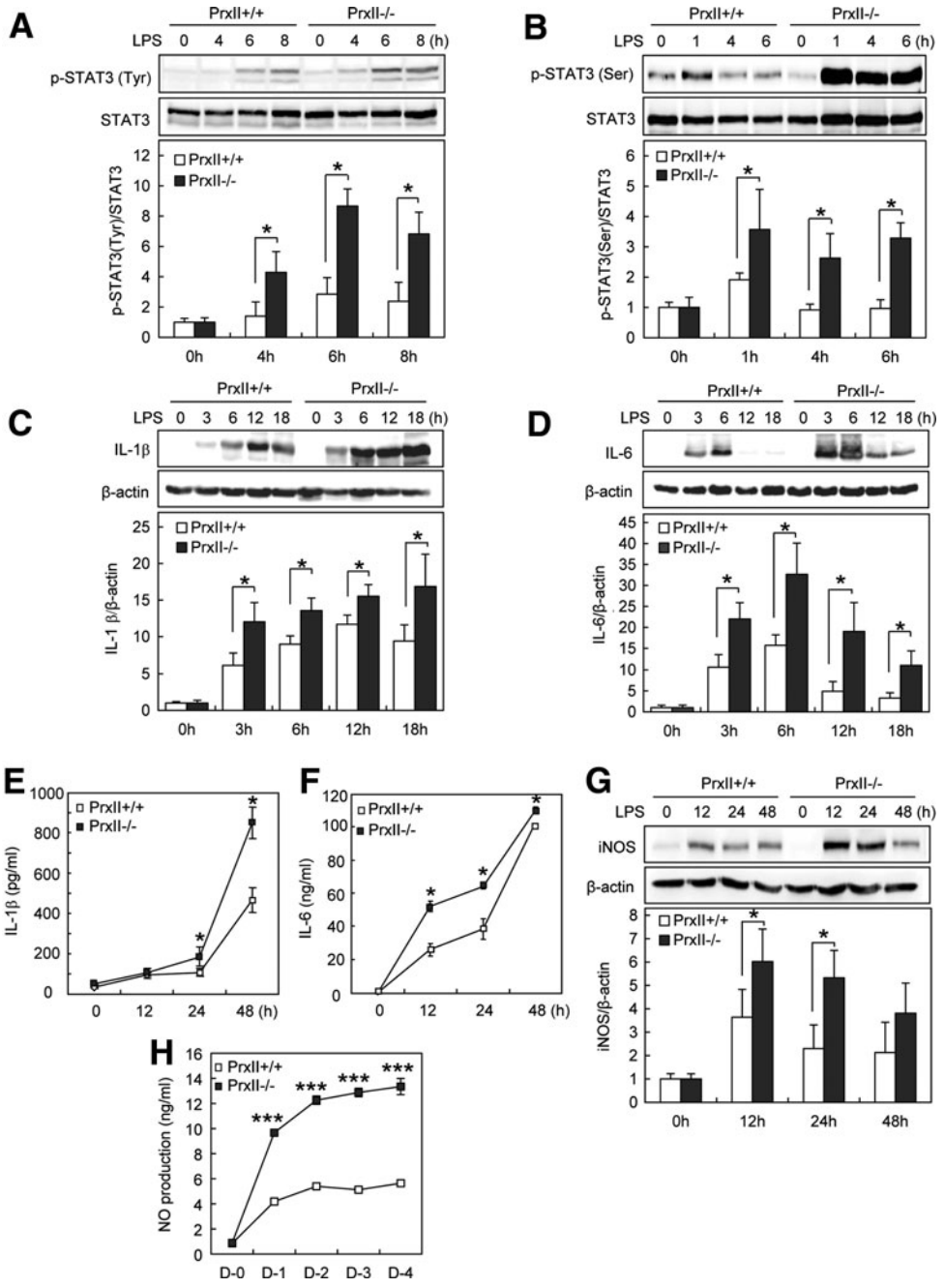

FIG. 6. PrxII deficiency promotes STAT3-mediated IL-1β, IL-6, and NO production during LPS-induced osteoclastogenesis. **(A, B)** Preosteoclasts were serum starved for 12 h and stimulated with 1 μg/ml LPS for the indicated time. Whole-cell extracts were harvested from cultured cells and subjected to SDS-PAGE and Western blot analysis to detect phosphorylated STAT3 at Tyr705 **(A)** and Ser727 **(B)**. Antibodies specific for STAT3 were used to normalize the cell extracts. **(C, D)** Preosteoclasts were serum starved for 12 h and stimulated with 1 μg/ml LPS for the indicated time. Whole-cell extracts were harvested from cultured cells and subjected to SDS-PAGE and Western blot analysis to detect IL-1β and IL-6. **(E, F)** Preosteoclasts were serum starved for 12 h and stimulated with 1 μg/ml LPS for the indicated time. IL-1β and IL-6 concentration was measured in cell supernatants using ELISA method. **(G)** Preosteoclasts were serum starved for 12 h and stimulated with 1 μg/ml LPS for the indicated time. After incubation, whole-cell extracts were harvested from cultured cells and subjected to SDS-PAGE and Western blot analysis to detect iNOS expression. **(H)** Preosteoclasts were stimulated with LPS for the indicated time, after which cell supernatants were harvested and NO production was measured as nitrite using the Griess reagent. The detection of β-actin in each sample serves as a loading control. Data represent the means ± SD of three independent experiments. $*p < 0.05$, $***p < 0.005$.

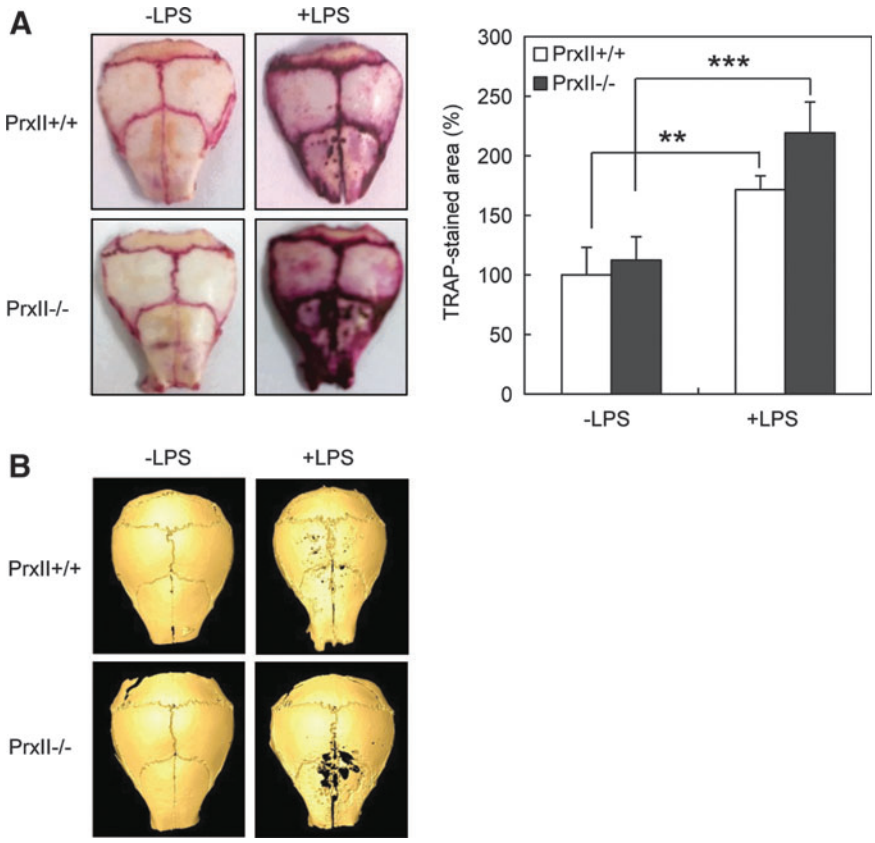

FIG. 7. PrxII-deficient mice show enhanced osteoclast formation by LPS *in vivo*. LPS or PBS was directly injected into calvariae. After 6 days, mice were sacrificed. **(A)** Extracted calvariae were fixed in 4% paraformaldehyde for 24 h at 4°C and then stained for TRAP. **(B)** Micro-CT images of whole calvariae are presented in which *dark spots* indicate eroded surfaces. $n=3$; $^{**}p<0.01$, $^{***}p<0.005$. PBS, phosphate-buffered saline.

mitochondrial electron transport chain is an important source of ROS in cells undergoing aerobic metabolism, and mitochondria are quite susceptible to oxidative damage, which can result in enhanced mitochondrial ROS production (3, 8). NADPH oxidase is also an important source of ROS in macrophages (5). A previous study has shown that NADPH oxidase and mitochondrion-dependent ROS generation may play important roles in PrxII regulation of LPS-induced inflammatory responses in macrophages (57). Thus, PrxII may regulate LPS-induced bone loss *via* NADPH oxidase and mitochondrial ROS generation. Further study is needed to reveal the precise mechanism by which PrxII regulates the LPS-induced bone loss in the context of ROS generation.

Next, we considered which signaling molecules affect PrxII-mediated ROS signaling in osteoclastogenesis. Several intracellular signals are essential for osteoclast formation, including NF-κB, JNK, ERK, and p38 MAPK. JNK activity, in particular, is required to maintain the committed status during osteoclastogenesis (9). We found that ROS mediate LPS-induced osteoclast formation *via* JNK (Fig. 1). Consistent with these results, lack of PrxII accelerated LPS-induced JNK phosphorylation, which results in the promotion of c-Fos and NFATc1 expression (Fig. 5). Lack of PrxII failed to exert any effects on NF-κB, ERK, and p38 MAPK (data not shown). These results suggest that PrxII regulates LPS-induced osteoclastogenesis through JNK-c-Fos-NFATc1 signaling pathways. Yang *et al.* have previously reported that LPS induces substantially enhanced activation of NF-κB and MAPK in PrxII-deficient macrophages (57). Given that the characteristics of RANKL-primed osteoclast precursors are different from those of macrophages (9, 33), PrxII-mediated signaling pathways seem to depend on the cell type.

Moreover, we identified another signaling molecule STAT3 that is critically involved in ROS signaling during LPS-induced osteoclastogenesis (Fig. 2). This study showed that LPS increases STAT3 phosphorylation *via* ROS in pre-osteoclasts. Our data verified that STAT3 regulates the LPS-induced expression of pro-inflammatory cytokines IL-1β and IL-6. In addition, STAT3 regulated the expression of iNOS and NO production by LPS (Fig. 3). IL-1β and IL-6 are known to be involved in the pathogenesis of diverse inflammatory disorders, including bone diseases (27, 44). Furthermore, pro-inflammatory cytokines have been known to produce NO (12), which may enhance osteoclastogenesis by mediating cell fusion (37). Thus, STAT3 might be involved in ROS-mediated signaling by LPS, which regulates cell–cell fusion to mature osteoclasts. Although the role of STAT3 in osteoclasts is somewhat controversial, many studies have demonstrated the importance of STAT3 in bone physiology. Protein inhibitor of activated STAT3 (PIAS3) has been known to negatively regulate RANKL-mediated osteoclastogenesis (19). Furthermore, knock-in gp130 mutant mice, which are unable to elicit gp130-dependent STAT1/3 activation, exhibit inhibited osteoclastogenesis (46). In osteoblasts, STAT3 activation leads to the production of RANKL for induction of osteoclastogenesis (38). These results support our suggestion that STAT3 activation by ROS plays a critical role in LPS-induced osteoclast formation. Furthermore, one of the most noteworthy findings of this study is that LPS-induced STAT3 signaling is dependent on

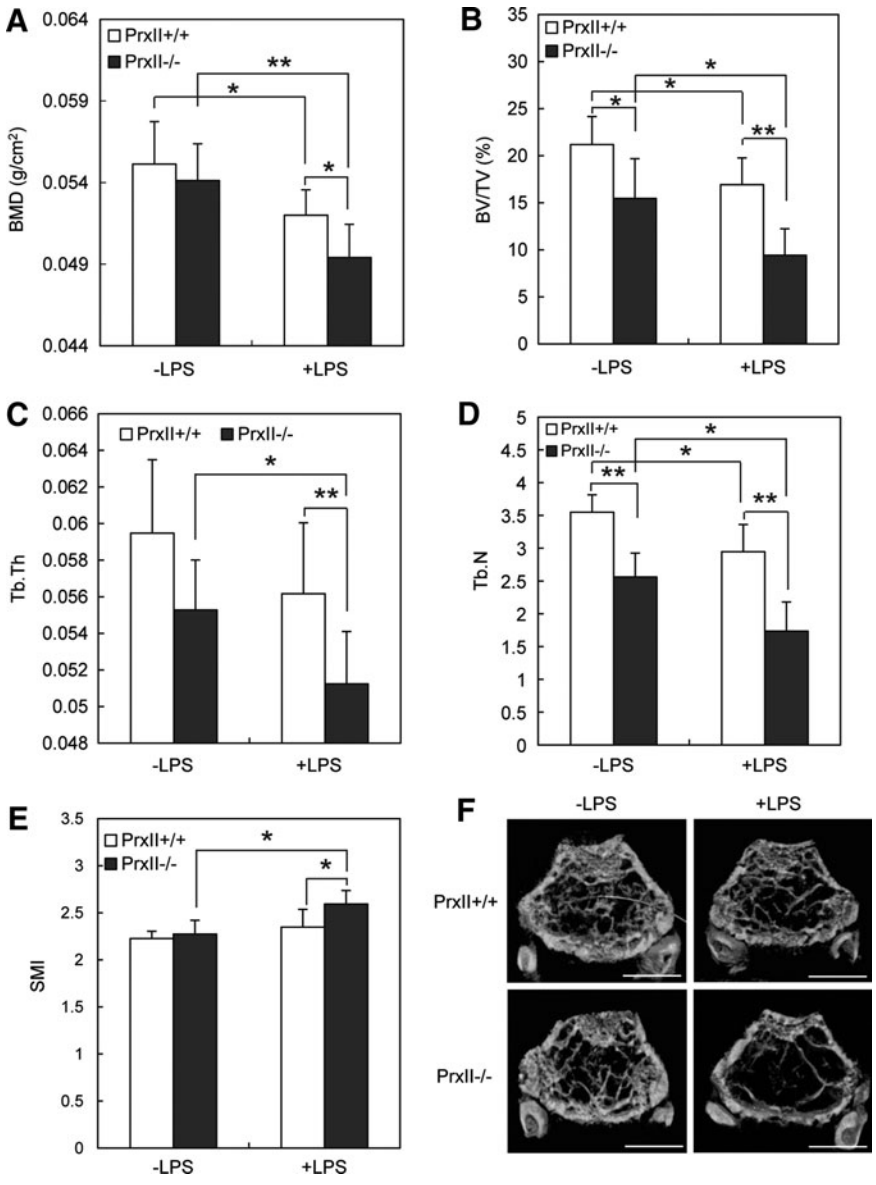

FIG. 8. PrxII-deficient mice show accelerated bone loss by LPS challenge. Twelve-week-old $PrxII^{+/+}$ and $PrxII^{-/-}$ mice were injected i.p. with 5 mg/kg LPS on days 0 and 4 and then sacrificed on day 8. **(A)** BMD (g/cm^2) of femur from $PrxII^{+/+}$ and $PrxII^{-/-}$ mice was analyzed by DXA. **(B–F)** BV/TV, % **(B)**, Tb.Th **(C)**, Tb.N **(D)**, SMI **(E),** and three-dimensional micro-CT images of the distal metaphyses of the femora **(F)**. $n=7$; $*p<0.05$, $**p<0.01$. Scale bar 1.0 mm. BMD, bone mineral density; BV/TV, bone volume per tissue volume; DXA, dual X-ray absorptiometry; SMI, structure model index; Tb.N, trabecular number; Tb.Th, trabecular thickness.

PrxII, which critically mediates the production of proinflammatory cytokines and NO (Fig. 6). Our study provides important insights into the involvement of PrxII-dependent STAT3 in LPS-induced osteoclastogenesis.

In summary, we verified that LPS-induced ROS signaling is dependent on the coordinated mechanism of JNK and STAT3, which is critically mediated by PrxII (Fig. 9). Several *in vitro* and *in vivo* studies have implicated PrxII as either a therapeutic target or a diagnostic biomarker for major diseases. For example, a previous study showing the specific involvement of PrxII in smooth muscle cell proliferation suggests the potential therapeutic use of PrxII for the inhibition of atherogenic lesion progression (10). In addition, PrxII has been identified as a novel predictive biomarker of the response to induction chemotherapy in patients with osteosarcoma (28). Our data imply the negative role of PrxII in the regulation of LPS-induced bone loss, which could be useful in the development of a novel treatment for patients with inflammatory bone loss.

Materials and Methods

Mouse models

PrxII knock-out mice were provided by Dr. Dae-Yeul Yu of the Korea Research Institute of Bioscience and Biotechnology (KRIBB). C3H/HeN mice (carrying wild-type TLR4) and C3H/HeJ mice (carrying mutated TLR4) were obtained from Central Lab. Animal, Inc. (Seoul, Korea). All mice were maintained in the animal facility of the Sookmyung Women's University on a 12:12-h light-dark cycle, and were allowed food and water *ad libitum*. All experiments were performed in accordance with institutional guidelines approved by the Sookmyung Women's University Animal Care and Use Committee.

Preparation of preosteoclasts

Total spleen cells were isolated from 12-week-old mice and cultured for 1 day in α-MEM (WelGENE, Inc., Daegu,

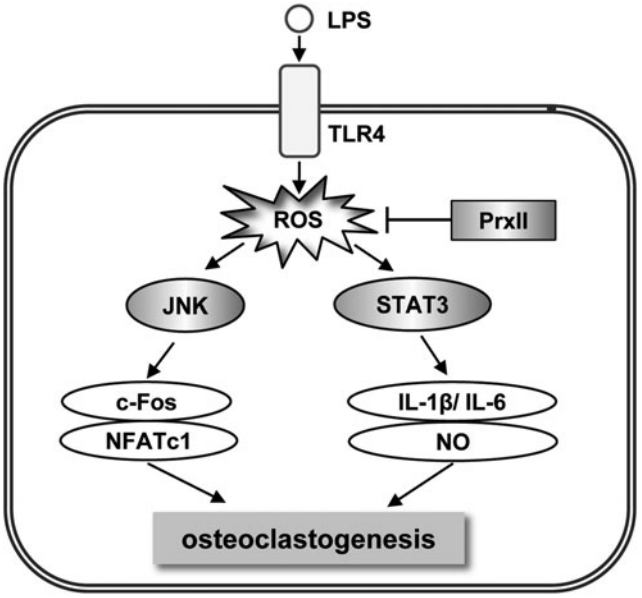

FIG. 9. A schematic model for the role of PrxII in LPS-induced osteoclastogenesis. In preosteoclast, PrxII inhibits ROS-mediated JNK and STAT3 activity, resulting in attenuation of osteoclastogenesis by LPS.

Korea) containing 10% fetal bovine serum (WelGENE) at 37°C in a humidified atmosphere under 5% CO_2. Nonadherent cells were collected and further cultured for 6 days in the presence of 30 ng/ml recombinant murine macrophage-colony-stimulating factor (rmM-CSF) (R&D Systems, Minneapolis, MN) (1). Adherent cells (osteoclast precursors) were cultured for an additional 1.5 days in 30 ng/ml rmM-CSF and 100 ng/ml mRANKL (PeproTech, Inc., Rocky Hill, NJ) to generate preosteoclasts.

Osteoclast differentiation in vitro

Preosteoclasts were plated into 96-well culture plates (1.5×10^4 cells/well) and cultured with 1 μg/ml LPS from *Escherichia coli* (Sigma-Aldrich, St. Louis, MO) in the presence of 30 ng/ml rmM-CSF. After 3–4 days in culture, TRAP staining was performed and TRAP-positive multinucleate cells with more than three nuclei were counted.

TRAP staining of osteoclasts

Osteoclasts were observed by staining tartrate-resistant acid phosphatase (TRAP) activity. Cultured cells were fixed with 10% formalin for 10 min, permeabilized with ethanol:acetone (50:50 v/v) for 1 min at room temperature, and incubated in acetate buffer (pH 5.2) containing naphthol AS-MX phosphate (Sigma-Aldrich) as the substrate and Fast Red Violet LB salt (Sigma-Aldrich) as the dye for the reaction product in the presence of 50 n*M* sodium tartrate. After washing with distilled water and drying, TRAP-positive MNCs ($n > 3$) were counted using a light microscope. The data were expressed as mean ± standard deviation (SD).

Bone resorption assay

Preosteoclasts were differentiated on dentin slices with rmM-CSF (30 ng/ml) and LPS (1 μg/ml) for 6 days. The cells were removed from the dentin slice by wiping its surface; then, slices were stained with toluidine blue (1 μg/ml; J.T. Baker, London, United Kingdom). The numbers of pits formed by bone resorption on the dentin slices were counted.

Retroviral gene transfer

To generate retroviral stocks, pMX-IRES-PrxII was transfected into the packaging cell line Plat-E. Viral supernatant was collected from culture media at 48 h after transfection. For infection with retroviruses, osteoclast precursors were incubated with the viral supernatant (4 ml/dish), polybrene (10 μg/ml) (Millipore, Billerica, MA), and rmM-CSF (30 ng/ml) for 2 day, and selected by puromycin (Sigma-Aldrich; 10 μg/ml) for an additional 48 h.

siRNA transfection

Osteoclast precursors were plated on 48-well plates at a density of 3.5×10^4 cells/well with 30 ng/ml rmM-CSF. After 24 h, cells were transfected with 100 n*M* mouse STAT3 on-target plus smart pool siRNAs (cat. No. L-040794-01-0005; accession numbers: NM_011486) (Dharmacon, Chicago, IL) using Lipofectamine 2000 (Invitrogen, Carlsbad, CA) according to the manufacturer's instructions. The control contained 100 n*M* nontargeting siRNA (Dharmacon). The transfection took place in 2.5 ml of serum free media for 6 h; the cells were then cultured for 1.5 days in complete media containing 30 ng/ml rmM-CSF and 100 ng/ml mRANKL to make preosteoclasts.

Immunoblot analysis

Cells were lysed in lysis buffer (50 m*M* Tris HCl, pH 7.5, 150 m*M* NaCl, 1% NP-40, 1 m*M* EDTA, 0.25% SDS, 1 m*M* NaF, 1 m*M* Na_3VO_4, 1 m*M* phenylmethylsulfonyl fluoride, pepstatin, leupeptin, and aprotinin) and were clarified by centrifugation. Protein was measured by Bradford assay (Bio-Rad Laboratories, Inc., Benicia, CA), and equal amounts of protein were separated on sodium dodecyl sulfate–polyacrylamide gel electrophoresis (SDS-PAGE) and transferred onto polyvinylidene fluoride (PVDF) membrane (Immobilon-P; Millipore). The membranes were blocked with 5% nonfat-milk in phosphate-buffered saline with 0.1% Tween 20 (PBS-T) and then immunostained with the indicated antibody. The membranes were developed using an enhanced chemiluminescence detection kit (Amersham Biosciences, Buckinghamshire, United Kingdom).

Antibodies

Specific antibodies against NFATc1, β-actin, and secondary horseradish peroxidase-IgG were obtained from Santa Cruz Biotechnology, Inc. (Santa Cruz, CA). Specific antibodies against IL-1β and IL-6 were purchased from R&D Systems. Others were purchased from Cell Signaling Technology (Irvine, CA). Each antibody was used at the concentration recommended by its manufacturer.

RNA extraction and real-time PCR assays

Total RNA was purified with easy-BLUE (iNtRON Biotechnology, Seoul, Korea), and cDNA was prepared from 1 μg of RNA using RevertAid First-Strand cDNA Synthesis

Kit (Fermentas, Hanover, MD). The PCR primer sequences used were as follows: CTR (F) 5′-TTTCAAGAACCTT AGCT GCCAGAG-3′, (R) 5′-CAAGGCACGGACAA TGT TGAGAAG-3′; CTK (F) 5′-ACGGAGGCATT GA CTCTGAAGATA-3′, (R) 5′-GTTGTTCTTATTCCGAGCC AAGAG-3′; ATP6v0d2 (F) 5′-TCAGATCT CTTCAA GGCTGTGCTG-3′, (R) 5′-GTGCC AAATGAGTTCAGA GTGATG-3′; DC-STAMP (F) 5′-TGGAAGTTCACTTG AAACTACGTG-3′, (R) 5′-CTCGGT TTCCCTCAGCCT CTCTC-3′; β3-Integrin (F) 5′-GATGACA TCGAGCAG GTGAAAGAG-3′, (R) 5′-CCGGTCATGAATGGTGATG AGTAG-3′; GAPDH (F) 5′-TGCACCACCAACTGCTTA GC-3′, (R) 5′-GGCATGGACTGTGGTCATGAG-3′. Real-time PCR reactions with the primers mentioned earlier were performed in a total volume of 20 μl using SYBR® Green PCR Master Mix (Applied Biosystems, Foster City, CA) according to the manufacturer's protocol. Thermocycling was performed using a 7500 Real-Time PCR System (Applied Biosystems) with the following conditions: initial hold 95°C for 10 min, followed by 40 cycles of denaturation at 95°C for 15 s, annealing at 58°C, and extension at 60°C for 1 min. Data were analyzed using 7500 System Sequence Detection Software version (Applied Biosystems). An index mRNA level was assessed using a threshold cycle (Ct) value and normalized against glyceraldehyde 3-phophate dehydrogenase (GAPDH) expression.

Enzyme-linked immunosorbent assay

Preosteoclasts were incubated with 30 ng/ml rmM-CSF and 1 μg/ml LPS for the indicated time, and cell supernatant was collected to determine the levels of IL-1β and IL-6 using a commercially available ELISA kit (Biolegend, San Diego, CA) according to the manufacturer's instructions. Assays were performed in triplicate for each specimen, and the data were converted to pg/ml or ng/ml.

Measurement of intracellular ROS

To monitor the intracellular ROS, 2′,7′-dichlorofluorescin-diacetate (DCFH-DA) (Sigma-Aldrich) were used as cell-permeable probes. Nonfluorescent DCFH-DA, hydrolyzed to DCFH inside of cells, yields highly fluorescent DCF in the presence of intracellular hydrogen peroxide and related peroxides. Preosteoclasts were washed once with PBS, then incubated in growth media containing 50 μM DCFH-DA for 30 min at 37°C, and finally incubated with 1 μg/ml LPS for the indicated time. DCF fluorescence was measured at an excitation wavelength of 488 nm and an emission of 515–540 nm.

Measurement of NO

Nitrite concentration was used as an assessment of NO production. Nitrite, a stable end-product of NO oxidation, was measured in cell culture supernatant by Griess assay. Preosteoclasts were incubated with 30 ng/ml rmM-CSF and 1 μg/ml LPS for the indicated time, and cell supernatant was collected to measure nitrite concentration using the Griess reaction by adding 100 μl of Griess reagent (0.1% naphthylethylene-diamide dihydrochloride in H_2O and 1% sulfanilamide in 5% concentrated phosphoric acid) to 100 μl of sample. Absorbance was then measured at 540 nm, and nitrite concentration was calculated by a comparison with sodium nitrite standards (5–80 μg/ml).

Osteoclast formation in vivo

To investigate the contribution of PrxII to LPS-induced osteoclast formation *in vivo*, 12-week-old $PrxII^{+/+}$ and $PrxII^{-/-}$ female mice were directly injected with 0.5 mg/mouse LPS on calvarial bone. After 6 days, mice were sacrificed; whole calvaria were fixed in 4% paraformaldehyde for 24 h and then stained with TRAP. Image analysis was accomplished by ImageJ software (version 1.32; National Institutes of Health, Bethesda, MD) according to the manufacturer's protocol.

Analysis of bone

$PrxII^{+/+}$ and $PrxII^{-/-}$ female mice (12-week old) were i.p. injected with LPS (5 mg/kg of body weight) on day 0 and 4. Mice in the control group were injected with saline only. On day 8, the femurs were collected. Isolated femurs were stored in 70% ethanol at 4°C until analysis. BMD (g/cm^2) of femurs was measured and analyzed by the dual X-ray absorptiometry (DXA) instrument PIXIMUS (GE Lunar, Madison, WI). Three-dimensional measurement was performed with a micro-CT scanner and associated analysis software (Model 1076; Skyscan, Antwerp, Belgium) at 9-mm voxel size. Image acquisition was performed at 35 kV of energy and 220 mA of intensity. The threshold was set to segment the bone from the background, and the same threshold setting was used for all samples.

Statistical analysis

The descriptive statistics provide data as the mean (SD). Means were compared with those of a Student's *t*-test (for comparison of two means) or an ANOVA (for multiple comparison) with a least-significant-difference *post hoc* test. A p-value < 0.05 was considered significant. Calculations were done with the software package SPSS (Ver. 21.0 for windows; SPSS, Inc., Chicago, IL).

Acknowledgments

This work was supported by the National Research Foundation of Korea (NRF) grant funded by the Korean government (MSIP) (MRC program, No. 2011-0030074), by the NRF grant (NRF-2010-616-E00013), and by the Basic Science Research Program through the NRF funded by the Ministry of Education, Science, and Technology (NRF-2009-0077185) for M.Y.

Author Disclosure Statement

No competing financial interests exist.

References

1. Alatery A and Basta S. An efficient culture method for generating large quantities of mature mouse splenic macrophages. *J Immunol Methods* 338: 47–57, 2008.
2. Aslan M and Ozben T. Oxidants in receptor tyrosine kinase signal transduction pathways. *Antioxid Redox Signal* 5: 781–788, 2003.
3. Balaban RS, Nemoto S, and Finkel T. Mitochondria, oxidants, and aging. *Cell* 120: 483–495, 2005.

4. Bhattacharyya J, Biswas S, and Datta AG. Mode of action of endotoxin: role of free radicals and antioxidants. *Curr Med Chem* 11: 359–368, 2004.
5. Bokoch G. Regulation of the phagocyte respiratory burst by small GTP-binding proteins. *Trends Cell Biol* 5: 109–113, 1995.
6. Boyle WJ, Simonet WS, and Lacey DL. Osteoclast differentiation and activation. *Nature* 423: 337–342, 2003.
7. Chae HZ, Chung SJ, and Rhee SG. Thioredoxin-dependent peroxide reductase from yeast. *J Biol Chem* 269: 27670–27678, 1994.
8. Chance B, Sies H, and Boveris A. Hydroperoxide metabolism in mammalian organs. *Physiol Rev* 59: 527–605, 1979.
9. Chang EJ, Ha J, Huang H, Kim HJ, Woo JH, Lee Y, Lee ZH, Kim JH, and Kim HH. The JNK dependent CaMK pathway restrains the reversion of committed cells during osteoclast differentiation. *J Cell Sci* 121: 2555–2564, 2008.
10. Choi MH, Lee IK, Kim GW, Kim BU, Han YH, Yu DY, Park HS, Kim KY, Lee JS, Choi C, Bae YS, Lee BI, Rhee SG, and Kang SW. Regulation of PDGF signalling and vascular remodelling by peroxiredoxin II. *Nature* 435: 347–353, 2005.
11. Cuzzocrea S, Mazzon E, Dugo L, Genovese T, Di Paola R, Ruggeri Z, Vegeto E, Caputi AP, Van De Loo FA, Puzzolo D, and Maggi A. Inducible nitric oxide synthase mediates bone loss in ovariectomized mice. *Endocrinology* 144: 1098–1107, 2003.
12. Daghigh F, Borghaei RC, Thornton RD, and Bee JH. Human gingival fibroblasts produce nitric oxide in response to proinflammatory cytokines. *J Periodontol* 73: 392–400, 2002.
13. Finkel T. Oxidant signals and oxidative stress. *Curr Opin Cell Biol* 15: 247–254, 2003.
14. Gyurko R, Shoji H, Battaglino RA, Boustany G, Gibson FC 3rd, Genco CA, Stashenko P, and Van Dyke TE. Inducible nitric oxide synthase mediates bone development and *P. gingivalis*-induced alveolar bone loss. *Bone* 36: 472–479, 2005.
15. Hadjidakis DJ and Androulakis II. Bone remodeling. *Ann N Y Acad Sci* 1092: 385–396, 2006.
16. Henderson B and Nair SP. Hard labour: bacterial infection of the skeleton. *Trends Microbiol* 11: 570–577, 2003.
17. Hensley K, Robinson KA, Gabbita SP, Salsman S, and Floyd RA. Reactive oxygen species, cell signaling, and cell injury. *Free Radic Biol Med* 28: 1456–1462, 2000.
18. Heymann D and Rousselle AV. Gp130 cytokine family and bone cells. *Cytokine* 12: 1455–1468, 2000.
19. Hikata T, Takaishi H, Takito J, Hakozaki A, Furukawa M, Uchikawa S, Kimura T, Okada Y, Matsumoto M, Yoshimura A, Nishimura R, Reddy SV, Asahara H, and Toyama Y. PIAS3 negatively regulates RANKL-mediated osteoclastogenesis directly in osteoclast precursors and indirectly *via* osteoblasts. *Blood* 113: 2202–2212, 2009.
20. Hoebe K, Du X, Georgel P, Janssen E, Tabeta K, Kim SO, Goode J, Lin P, Mann N, Mudd S, Crozat K, Sovath S, Han J, and Beutler B. Identification of Lps2 as a key transducer of MyD88-independent TIR signalling. *Nature* 424: 743–748, 2003.
21. Hofbauer LC, Khosla S, Dunstan CR, Lacey DL, Boyle WJ, and Riggs BL. The roles of osteoprotegerin and osteoprotegerin ligand in the paracrine regulation of bone resorption. *J Bone Miner Res* 15: 2–12, 2000.
22. Hotokezaka H, Sakai E, Ohara N, Hotokezaka Y, Gonzales C, Matsuo K, Fujimura Y, Yoshida N, and Nakayama K. Molecular analysis of RANKL-independent cell fusion of osteoclast-like cells induced by TNF-alpha, lipopolysaccharide, or peptidoglycan. *J Cell Biochem* 101: 122–134, 2007.
23. Jonas N and Elias SJA. Reactive oxygen, antioxidants, and the mammalian thioredoxin system. *Free Radic Biol Med* 31: 1287–1312, 2001.
24. Jules J, Zhang P, Ashley JW, Wei S, Shi Z, Liu J, Michalek SM, and Feng X. Molecular basis of requirement of receptor activator of nuclear factor κB signaling for interleukin 1-mediated osteoclastogenesis. *J Biol Chem* 287: 15728–15738, 2012.
25. Kim JH, Jin HM, Kim K, Song I, Youn BU, Matsuo K, and Kim N. The mechanism of osteoclast differentiation induced by IL-1. *J Immunol* 183: 1862–1870, 2009.
26. Kim MS, Yang YM, Son A, Tian YS, Lee SI, Kang SW, Muallem S, and Shin DM. RANKL-mediated reactive oxygen species pathway that induces long lasting Ca2+ oscillations essential for osteoclastogenesis. *J Biol Chem* 285: 6913–6921, 2010.
27. Kimble R, Srivastava S, Ross FP, Matayoshi A, and Pacifici R. Estrogen deficiency increases the ability of stromal cells to support murine osteoclastogenesis *via* an interleukin-1 and tumor necrosis factor-mediated stimulation of macrophage colony-stimulating factor production. *J Biol Chem* 271: 28890–28897, 1996.
28. Kubota D, Mukaihara K, Yoshida A, Tsuda H, Kawai A, and Kondo T. Proteomics study of open biopsy samples identifies peroxiredoxin 2 as a predictive biomarker of response to induction chemotherapy in osteosarcoma. *J Proteomics* 91: 393–404, 2013.
29. Kudo O, Sabokbar A, Pocock A, Itonaga I, Fujikawa Y, and Athanasou NA. Interleukin-6 and interleukin-11 support human osteoclast formation by a RANKL-independent mechanism. *Bone* 32: 1–7, 2003.
30. Lander HM. An essential role for free radicals and derived species in signal transduction. *FASEB J* 11: 118–124, 1997.
31. Lee ZH and Kim HH. Signal transduction by receptor activator of nuclear factor kappa B in osteoclasts. *Biochem Biophys Res Commun* 305: 211–214, 2003.
32. Lee TH, Kim SU, Yu SL, Kim SH, Park DS, Moon HB, Dho SH, Kwon KS, Kwon HJ, Han YH, Jeong S, Kang SW, Shin HS, Lee KK, Rhee SG, and Yu DY. Peroxiredoxin II is essential for sustaining life span of erythrocytes in mice. *Blood* 101: 5033–5038, 2003.
33. Mochizuki A, Takami M, Kawawa T, Suzumoto R, Sasaki T, Shiba A, Tsukasaki H, Zhao B, Yasuhara R, Suzawa T, Miyamoto Y, Choi Y, and Kamijo R. Identification and characterization of the precursors committed to osteoclasts induced by TNF-related activation-induced cytokine/receptor activator of NF-kappa B ligand. *J Immunol* 177: 4360–4368, 2006.
34. Moon EY, Noh YW, Han YH, Kim SU, Kim JM, Yu DY, and Lim JS. T lymphocytes and dendritic cells are activated by the deletion of peroxiredoxin II (PrxII) gene. *Immunol Lett* 102: 184–190, 2006.
35. Nagasawa T, Kiji M, Yashiro R, Hormdee D, Lu H, Kunze M, Suda T, Koshy G, Kobayashi H, Oda S, Nitta H, and Ishikawa I. Roles of receptor activator of nuclear factor-kappaB ligand (RANKL) and osteoprotegerin in periodontal health and disease. *Periodontol 2000* 43: 65–84, 2007.
36. Nair SP, Meghji S, Wilson M, Reddi K, White P, and Henderson B. Bacterially induced bone destruction: mechanism and misconceptions. *Infect Immun* 64: 2371–2380, 1996.

37. Nilforoushan D, Gramoun A, Glogauer M, and Manolson MF. Nitric oxide enhances osteoclastogenesis possibly by mediating cell fusion. *Nitric Oxide* 21: 27–36, 2009.
38. O'Brien CA, Gubrij I, Lin SC, Saylors RL, and Manolagas SC. STAT3 activation in stromal/osteoblastic cells is required for induction of the receptor activator of NF-κB ligand and stimulation of osteoclastogenesis by gp130-utilizing cytokines or interleukin-1 but not 1,25-dihydroxyvitamin D3 or parathyroid hormone. *J Biol Chem* 274: 19301–19308, 1999.
39. Pawate S, Shen Q, Fan F, and Bhat NR. Redox regulation of glial inflammatory response to lipopolysaccharide and interferongamma. *J Neurosci Res* 77: 540–551, 2004.
40. Poltorak A, He X, Smirnova I, Liu MY, Van Huffel C, Du X, Birdwell D, Alejos E, Silva M, Galanos C, Freudenberg M, Ricciardi-Castagnoli P, Layton B, and Beutler B. Defective LPS signaling in C3H/HeJ and C57BL/10ScCr mice: mutations in Tlr4 gene. *Science* 282: 2085–2088, 1998.
41. Rhee SG, Chae HZ, and Kim K. Peroxiredoxins: a historical overview and speculative preview of novel mechanisms and emerging concepts in cell signaling. *Free Radic Biol Med* 38: 1543–1552, 2005.
42. Rhee SG and Woo HA. Multiple functions of peroxiredoxins: peroxidases, sensors and regulators of the intracellular messenger H(2)O(2), and protein chaperones. *Antioxid Redox Signal* 15: 781–794, 2011.
43. Rhee SG, Woo HA, Kil IS, and Bae SH. Peroxiredoxin functions as a peroxidase and a regulator and sensor of local peroxides. *J Biol Chem* 287: 4403–4410, 2012.
44. Roland A, Christina B, Gerhard K, Jochen Z, Josef S, and Georg S. Inhibition of interleukin-6 receptor directly blocks osteoclast formation *in vitro* and *in vivo*. *Arthritis Rheum* 60: 2747–2756, 2009.
45. Samavati L, Rastogi R, Du W, Hüttemann M, Fite A, and Franchi L. STAT3 tyrosine phosphorylation is critical for interleukin 1 beta and interleukin-6 production in response to lipopolysaccharide and live bacteria. *Mol Immunol* 46: 1867–1877, 2009.
46. Sims NA, Jenkins BJ, Quinn JM, Nakamura A, Glatt M, Gillespie MT, Ernst M, and Martin TJ. Glycoprotein 130 regulates bone turnover and bone size by distinct downstream signaling pathways. *J Clin Invest* 113: 379–389, 2004.
47. Suda K, Woo JT, Takami M, Sexton PM, and Nagai K. Lipopolysaccharide supports survival and fusion of preosteoclasts independent of TNF-alpha, IL-1, and RANKL. *J Cell Physiol* 190: 101–108, 2002.
48. Sun J, Ramnath RD, Zhi L, Tamizhselvi R, and Bhatia M. Substance P enhances NF-kappaB transactivation and chemokine response in murine macrophages *via* ERK1/2 and p38 MAPK signaling pathways. *Am J Physiol Cell Physiol* 294: C1586–C1596, 2008.
49. Takahashi N, Udagawa N, and Suda T. A new member of tumor necrosis factor ligand family, ODF/OPGL/TRANCE/RANKL, regulates osteoclast differentiation and function. *Biochem Biophys Res Commun* 256: 449–455, 1999.
50. Takayanagi H. The role of NFAT in osteoclast formation. *Ann N Y Acad Sci* 1116: 227–237, 2007.
51. Tonks NK. Redox redux: revisiting PTPs and the control of cell signaling. *Cell* 121: 667–670, 2005.
52. Torres M. Mitogen-activated protein kinase pathways in redox signaling. *Front Biosci* 8: d369–d391, 2003.
53. Wauquier F, Leotoing L, Coxam V, Guicheux J, and Wittrant Y. Oxidative stress in bone remodelling and disease. *Trends Mol Med* 15: 468–477, 2009.
54. Wood ZA, Schroder E, Harris JR, and Poole LB. Structure, mechanism and regulation of peroxiredoxins. *Trends Biochem Sci* 28: 32–40, 2003.
55. Yamamoto M, Sato S, Hemmi H, Sanjo H, Uematsu S, Kaisho T, Hoshino K, Takeuchi O, Kobayashi M, Fujita T, Takeda K, and Akira S. Essential role for TIRAP in activation of the signalling cascade shared by TLR2 and TLR4. *Nature* 420: 324–329, 2002.
56. Yamamoto M, Sato S, Hemmi H, Uematsu S, Hoshino K, Kaisho T, Takeuchi O, Takeda K, and Akira S. TRAM is specifically involved in the Toll-like receptor 4-mediated MyD88-independent signaling pathway. *Nat Immunol* 4: 1144–1150, 2003.
57. Yang CS, Lee DS, Song CH, An SJ, Li A, Kim JM, Kim CS, Yoo DG, Jeon BH, Yang HY, Lee TH, Lee ZW, Jamel E, Yu DY, and Jo EK. Roles of Peroxiredoxin II in the regulation of proinflammatory responses to LPS and protection against endotoxin-induced lethal shock. *J Exp Med* 204: 583–594, 2007.
58. Yang X, Ricciardi BF, Hernandez-Soria A, Shi Y, Pleshko Camacho N, and Bostrom MP. Callus mineralization and maturation are delayed during fracture healing in interleukin-6 knockout mice. *Bone* 41: 928–936, 2007.
59. Zou W and Bar-Shavit Z. Dual modulation of osteoclast differentiation by lipopolysaccharide. *J Bone Miner Res* 17: 1211–1218, 2002.

Address correspondence to:
Prof. Mijung Yim
College of Pharmacy
Sookmyung Women's University
Hyochangwongil 52
Seoul 140-742
Republic of Korea

E-mail: myim@sm.ac.kr

Prof. Dong-Seok Lee
College of Natural Sciences
Kyungpook National University
Daegu 702-701
Republic of Korea

E-mail: lee1@knu.ac.kr

Date of first submission to ARS Central, November 19, 2013; date of final revised submission, July 9, 2014; date of acceptance, July 30, 2014.

Abbreviations Used

ATP6v0d2 = V-ATPase d2
BMD = bone mineral density
BV/TV = bone volume per tissue volume
CREB = cAMP response element-binding protein
CTK = cathepsin K
CTR = calcitonin receptor
DC-STAMP = dendritic cell-specific transmembrane protein

Abbreviations Used (Cont.)

DXA = dual X-ray absorptiometry
ELISA = enzyme-linked immunosorbent assay
ERK1/2 = extracellular signal-regulated kinase 1/2
GAPDH = glyceraldehyde 3-phophate dehydrogenase
IL-1β = interleukin-1 beta
IL-6 = interleukin-6
iNOS = inducible nitric oxide synthase
JNK = c-Jun N-terminal protein kinase
LPS = lipopolysaccharide
MAPK = mitogen-activated protein kinase
M-CSF = macrophage-colony-stimulating factor
MNCs = multinucleated cells
MyD88 = myeloid differentiation primary response gene 88
NAC = *N*-acetyl-cysteine
NFATc1 = nuclear factor of activated T-cells, cytoplasmic 1
NF-κB = nuclear factor-kappaB
NO = nitric oxide
PBS-T = phosphate-buffered saline with 0.1% Tween 20
PCR = polymerase chain reaction
PIAS3 = protein inhibitor of activated STAT3
PLCγ-1 = phospholipase-C gamma-1
PrxII = peroxiredoxin II
Prxs = peroxiredoxins
RANK = receptor activator of nuclear factor-kappaB
RANKL = receptor activator of nuclear factor-kappaB ligand
rmM-CSF = recombinant murine macrophage-colony-stimulating factor
ROS = reactive oxygen species
SD = standard deviation
SDS-PAGE = sodium dodecyl sulfate–polyacrylamide gel electrophoresis
siRNA = small interfering RNA
SMI = structure model index
STAT3 = signal transducer and activator of transcription 3
Tb.N = trabecular number
Tb.Th = trabecular thickness
TIR = toll-interleukin-1 receptor
Tirap = toll-interleukin 1 receptor domain containing adaptor protein
TLR4 = toll-like receptor 4
TNF = tumor necrosis factor
TRAF-6 = TNF receptor-associated factor 6
Tram = TRIF-related adaptor molecule
TRAP = tartrate-resistant acid phosphatase
Trif = TIR-domain-containing adapter-inducing interferon-β